







Design and Integration of a Low-Back Exoskeleton: A 3D-Printed Cycloidal Drive Actuator for Flexible Human-Robot Interaction.

Gabriele Gambirasio¹, Mattia Pesenti¹ , Mattia Panzenbeck¹, Marta Gandolla¹ , Loris Roveda² ,
Mario Covarrubias¹ 

¹Politecnico di Milano, Italy,

²Istituto Dalle Molle di studi sull'Intelligenza Artificiale (IDSIA), Scuola Universitaria Professionale della Svizzera Italiana (SUPSI), Università della Svizzera italiana (USI), via la Santa 1, 6962, Lugano, Switzerland
loris.roveda@idsia.ch,

Corresponding author: Mario Covarrubias, mario.covarrubias@polimi.it

Abstract. In the last decades, the adoption of assistive devices has been spreading among different application fields, starting from the rehabilitative medicine to the industrial field. In particular, exoskeletons aimed to ease the operations performed by workers have been developed in order to reduce the entity of work-related musculoskeletal disorders, limiting the inconvenience caused to the workers and reducing therapy-related costs faced by the employer or the healthcare system. However, commercial full-body exoskeletons equipped with efficient, low-weight actuation systems require a huge investment (both for purchase and maintenance), which only a few companies are willing to pay. In order to achieve high performance while limiting costs and complexity, a custom cycloidal reduction was designed: because of its back-drivability and scalability, it represents a low-cost solution capable of maximizing the overall performances of the assistive device. In this paper, the methodology to define a custom low-cost yet efficient cycloidal drive actuation is hence proposed, as well as its implementation in the design of a low-back exoskeleton based on backbone kinematics.

Keywords: low-back exoskeleton, cycloidal transmission, back-drivable reduction, fast prototyping, additive manufacturing, FEM.

DOI: <https://doi.org/10.14733/cadaps.2024.791-806>

1 INTRODUCTION

In the last decades in the industrial field higher attention has been directed towards assistive devices. Initially developed in the military field to augment the wearer's strength and endurance, they quickly spread also in healthcare as a rehabilitative tool, in particular for helping stroke patients to recover mobility and dexterity [3]. It was in 2004, with the foundation of Cyberdyne, that the first commercial exoskeleton made its appearance:

the Robot Suit Hybrid Assistive Limb (HAL) provided the first solution as support to workers while performing repetitive tasks for a long time. Both the company and the workers were able to benefit from the adoption of this kind of equipment: by assisting the worker in wearing operations it is possible to reduce the occurrence and the entity of work-related musculoskeletal disorders, decreasing the risk for the user of becoming invalid and limiting the costs to be faced by the employer or the healthcare system. However, while providing support to the whole body of the user, the HAL is also rather expensive (its cost ranges from \$11,000 to \$19,000, while the rent has a monthly subscription of nearly \$1,000 [9]). Cost is often the major factor in reducing large-scale exoskeleton adoption.

In order to overcome this economic issue, some strategies have been developed to provide exoskeletons suitable for a wider range of applications and accommodate the needs of a larger number of customers. In the first place, exoskeletons acting only on a certain part of the user's body have been developed: lower limb exoskeletons like the Lokomat [8] were initially developed to assist the gait of stroke patients on a treadmill, while lower-back exoskeletons were designed mainly to relieve the back pain which could affect the workers subject to frequent payload manipulation. The reduced number of elements and the simpler design allow to reduce in a sensible way the cost of prototyping and manufacturing.

Subsequently, different actuation systems were considered and applied, providing different performances depending on the user's request. Passive devices rely on the adoption of elastic elements (like springs) to guarantee a simple and lighter design of the exoskeleton. On the other hand, powered systems can enhance the beneficial effects provided to the user, being more flexible and allowing the assistance to be tuned depending on the load to be lifted. Nevertheless, they have higher costs and complexity. Finally, hybrid actuation systems (made of both elastic elements and motors) can be employed in order to combine the benefits of the above-mentioned systems.

While the development of a passive actuation system is relatively easier, the shift towards active exoskeletons represents a more challenging topic, both in terms of mechanical design and control. Mounting of the actuation system is subject to different kinds of constraints (components' shape, dimensions, positioning, weight, ...), which must be respected in order to guarantee the exoskeleton is comfortable to be used and sufficiently light to be worn for a long period (i.e., a working shift).

In this work, the passive low-back exoskeleton presented in [6] has been considered as a starting point for the development of an active exoskeleton. The focus was aimed at the definition of an actuation system (motor+reducer) suitable for the application and the re-design of the exoskeleton in order to provide the required mechanical resistance, minimizing the encumbrance and the weight of the device. Thus, the first objective of this work is the design and development of a fully-3D-printed speed reducer to couple to a brushless DC (BLCD) motor. The second objective is coupling the aforementioned actuator with the scissor-hinge mechanism of the low-back exoskeleton mentioned above. Finally, the last objective is the re-design of the exoskeleton itself in order to fit the actuators and all the hardware required for its functioning (control boards, sensors, battery, ...).

The remaining of this manuscript is structured as follow. Section 2 describes the starting point, i.e., the low-back exoskeleton with passive actuation. Section ?? provides an overview of the actuating system (i.e., motor and transmission) that could be implemented on the exoskeleton and a particular focus on the development of a custom reduction suitable for the current application. Section 3 describes the step-by-step development of the new prototype, designed with the software Autodesk Inventor, presenting all the justifications for the decisions made during this phase. Eventually, the Section ?? concerns the simulations performed in order to validate the final prototype, both considering its kinematic and its mechanical behaviour.

2 PRELIMINARY DESIGN

The passive exoskeleton presented in [6] has been performed on the basis of the anthropometric tables presented in [4], considering data related to the 75th percentile for male subjects. Its functioning is rather simple. It is



Figure 1: Operating principle of a low-back exoskeleton based on backbone kinematics.

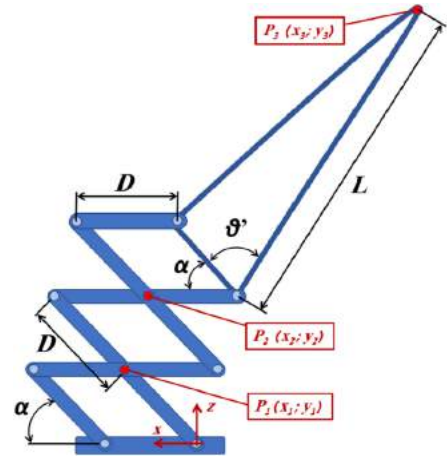


Figure 2: Scissor hinge configuration.

composed of two parts: the bottom one (hip support) is constrained to the lumbar part of the user, and the upper part (the moving part) is constrained to the wearer's back. The two parts are connected by a couple of identical scissor hinges and by a traction spring: when the user bends forward the potential (gravitational) energy of the torso is converted into potential (elastic) energy by extending the spring. This energy is then exploited by the exoskeleton when the user goes back to the straight position, thanks to the elastic force that pulls the upper part of the torso. Besides the elastic component, this device presents other crucial components: the interfaces between the user and the exoskeleton guarantee the correct transmission of the assistive force. Thus, they must be kept in consideration while designing the active version of the exoskeleton.

2.1 Scissor Hinge Mechanism

In order for the exoskeleton to work correctly, it needs to adapt to the back of the user when bending forward. In order to guarantee this behavior a scissor hinge mechanism (Figure 2) capable to follow the backbone kinematics has been developed as presented in [7].

The human backbone is made of 33 vertebrae distributed from the base of the skull to the pelvis, where 24 of them are articulated and named accordingly to their position: 7 cervical (C1-C7), 12 thoracics (T1-T12), 5 lumbar (L1-L5), 5 sacral (S1-S5) and 3 to 5 coccygeal vertebrae. Their relative movement during the forward bending of a person was acquired through a stereophotogrammetric system capable of recognizing the motion of markers applied in correspondence with the vertebrae. The recorded positions of the markers during the execution of the protocol were then processed in order to define circular paths that approximate the motion path of the vertebrae, shown in Figure 3. Finally, a 1-DoF scissor hinge mechanical system was designed in order to follow the motion of the T2 vertebra along its approximated circular trajectory (Figure 4). This design has been derived considering the kinematic of 3 points of interest (the revolute joints P_1 and P_2 and the final point P_3 of the mechanism, corresponding to the T2 vertebra):

$$\begin{cases} z_1 = D \cdot \sin(\alpha); \\ x_1 = D \cdot \cos(\alpha); \end{cases} \quad (1)$$

$$\begin{cases} z_2 = D \cdot \sin(\alpha) + z_1; \\ x_2 = D \cdot \cos(\alpha) - D + x_1; \end{cases} \quad (2)$$

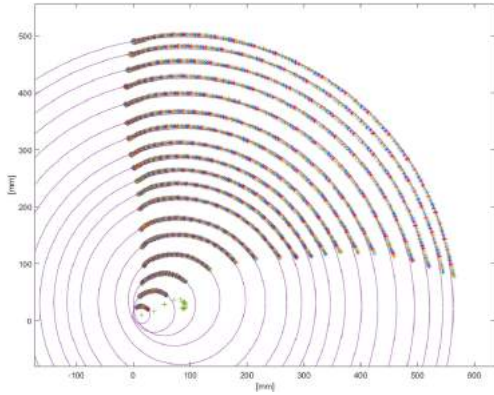


Figure 3: Circular approximation of the motion path of the vertebrae.

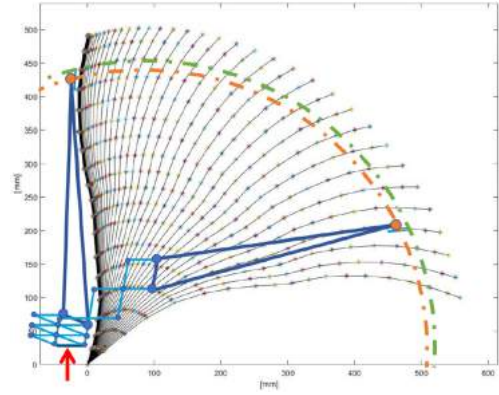


Figure 4: Comparison between the mechanism motion (yellow) and vertebra T2 motion (green). The red arrow represents the constraint between the mechanism and the lumbar fixing.

$$\begin{cases} z_3 = L \cdot \sin(\alpha + \theta') + z_2; \\ x_3 = D \cdot \cos(\alpha + \theta') - D + x_2. \end{cases} \quad (3)$$

This mechanical system represents the core element of the exoskeleton and must be kept while designing the following versions of the low-back exoskeleton. Changes to one or more parts can be applied to better adapt to the characteristic of the user (height, weight, ...), but these modifications must be consistent with the equations 1, 2 and 3.

2.2 User-exoskeleton Interface

In order to prototype an exoskeleton capable of adapting to different anthropometries, different sizes for hip-to-shoulder wearability have been defined in order to adapt to the height that different users can present. The interface has been achieved by means of soft links: backpack-like straps have been implemented for the shoulder constraints, at the waist was added an ergonomic belt, while for the lower limbs, elastic bands were added to the leg bars, guaranteeing sufficient comfort when wearing the device.

2.2.1 State of the art

A common choice is the Harmonic Drive reductions: thought being expensive, thanks to its compact design and to high performance (single stage, zero backlash, reliability, etc.) these components allow to obtain the required torque with minimal losses in power transmission. This solution is suitable for every kind of assistive device, like HAL (Hybrid Assistive Limb) by Cyberdyne or the upper limb exoskeleton CLEVERarm [2]. Thanks to the high reduction ratio and the high efficiency provided, it is possible to achieve high action forces even by adopting motors with low peak torque. However when it comes to low-volume prototypes, this choice becomes unfeasible due to high costs.

For assisting devices that require low forces (e.g. wrist exoskeletons) the adoption of the reduction can be avoided by mounting multiple motors with a direct actuation (RiceWrist [1]).

A different solution is the implementation of cost-effective, multistage motor reductions. This is the case of the HALEX (Human Assistive Lower limb EXoskeleton [11]): the multi-stage approach results in a dramatic

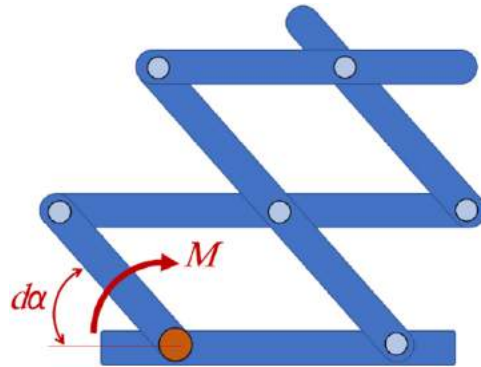


Figure 5: Actuation of the scissor hinge.

reduction of the efficiency, while size constraints force a limit on the reduction ratio.

A third solution is instead represented by a custom single-stage reduction designed to be cost-effective yet efficient, capable to provide the desired mechanical properties also adapting the size of the component to the current application.

2.2.2 Planetary gear reduction

A first custom reduction has been designed following the principles of the planetary gear reduction. A planetary gear is a system made of three kind of elements (Figure 6):

1. One gear placed in the center, called Sun gear;
2. At least three intermediary gears, called Planet pinion gears;
3. One external gear, toothed on the inside part, called Ring gear.

The name of this mechanism derives from the solar system: the planet gears rotate around the sun gear, which is at the center of the device, following with their axes a circular orbit. The planet pinions mesh both with the teeth of the sun gear and with the internal tooth ring gear and the constant mesh of all gears in the assembly guarantees its functioning. The performance of the planetary gear depends on the chosen configuration, i.e. on the gears used as input, output or kept fixed in position:

1. Fixing the ring gear, the sun gear is the input and the planet gears are the output (or vice versa);
2. Fixing the planet gears, the sun gear is the input and the ring gear is the output (or vice versa);
3. Fixing the sun gear, the planet gears are the input and the ring gear is the output (or vice versa).

In order to design a planetary reduction for the current application, the configuration with the ring gear fixed is the most convenient: expecting to prototype an external case capable of containing and protecting all the movable elements of the reduction, it is not difficult to realize anchor points in order to constrain the external gear (Figure 7). In this way, the sun gear can be directly joined to the BL electric motor, while a carrier can be constrained through pin joints (i.e. low-friction bearings) to the center of the planetary gears: the power exerted by the motor flows of the motor flows from the sun gear to the planet gears and, finally, to the carrier, the output of the reduction system.

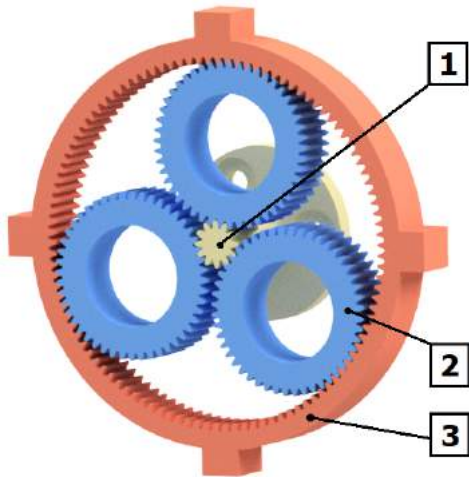


Figure 6: Design of a planetary gear:

- 1) Sun gear;
- 2) Planet pinion gear;
- 3) Ring gear.

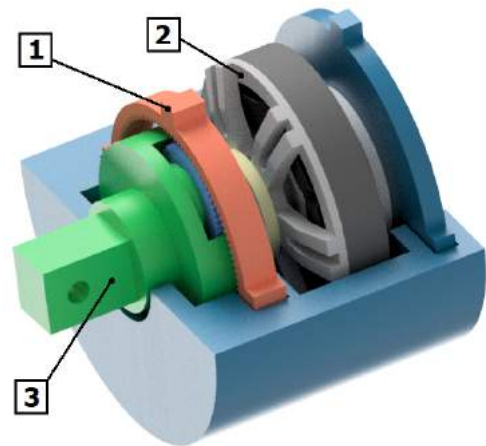


Figure 7: Assembly of the planetary reduction:

- 1) Planetary gear;
- 2) Brushless motor;
- 3) Carrier.

The reduction ratio of the mechanism depends on the configuration but it is always defined starting from the Willis equation, also called the fundamental equation for epicyclic gears [10]. Being n_i and d_i respectively the rotational speed and the pitch circle diameter of the gear i (where i can assume the values s for the sun gear, p for the planet gear and r for the ring gear), the equation can be derived in the following form:

$$n_p - d_p = n_c \cdot (d_p + d_s) - n_s \cdot d_s \quad (4)$$

After some consideration on the geometry of the reduction, the transmission ratio i from the sun gear (input) to the carrier (output) can be expressed as:

$$i = 1 + \frac{d_r}{d_s} \quad (5)$$

However it is possible to prove that the maximum reduction ratio achievable with a single-stage planetary gear is 10:1; this prevents the prototyping of a single stage transmission 30:1 exploiting this mechanism. In order to overcome this issue, a multi-stage transmission can be designed by introducing a second planetary gear downstream of the first one or by adding a spur gear coupled with the carrier (properly tuning the dimension of both components). The latter solution (Figure 8) in particular is less bulky and thus more suitable for the current application, even if higher attention must be paid in adding this second element: differently from the planetary gear where the presence of multiple planet gears generates opposite forces on the mechanism (preventing the bending of the motor axis), the spur gear introduces a force perpendicular to the rotational axis of the transmission which could bring to deformation of the components and to a lack in the meshing between the added gear and the carrier.

Moreover, the available volume on the exoskeleton must be considered: it has been evaluated that the reduction must have a radial dimension not bigger than 100mm. This limit causes the teeth of the gears to be very small (approximately 1 mm): this level of detail is difficult to achieve since it is desirable to produce all the custom components through 3D printing.

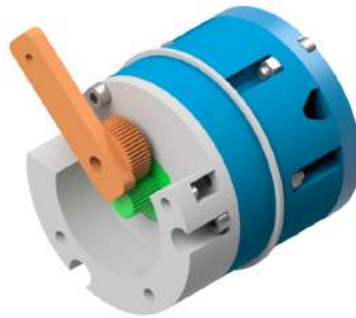


Figure 8: Planetary gear reduction assembly.

2.2.3 Cycloidal gear reduction

A second, custom solution is the one exploiting a contracted cycloidal gear. In order to understand its functioning, let's consider a disk (diameter $d = 2r$) placed inside a fixed ring characterized by an inner diameter defined as $D = 2R = d + E$, where e is an arbitrary value ($E \ll d$). Let's also consider a shaft with an eccentricity e mounted by means of a roller bearing in the middle of the disk, in order for the disk to have a contact point in common with the external ring. When the shaft rotates around its axis with a given angular speed, the disk is forced to "oscillate" around its center of gravity: thanks to the friction generated between this body and the ring, the disk starts to roll without slipping along the inner surface of the ring with a lower angular speed lower (in modulus) and opposite direction with respect to the one of the shaft. In order to generate an output torque coaxial with the input shaft some circular holes can be created in the disk: an equal number of pins, mounted onto an output plate, are inserted inside these cavities so that they are tangent to the lateral surfaces of the holes. When the disk rolls, the cavities start pushing the pins, causing the output plate to rotate axially to the input shaft with a lower angular speed. In order to exploit this working principle inside a transmission, a more reliable interaction between the disk and the outer cavity must be defined. Indeed, high torques, way higher than the friction forces present in the system, have to be transmitted from the input shaft to the output plate through the disk/ring interface. In order to overcome this issue, the shape of the disk is changed into a cycloidal gear.

In geometry, a cycloid is the curve traced by a point on a circle as it rolls along a straight line without slipping. It is also possible to make the circle rotate along the external circumference of the disk, while considering the track left by an enlargement of the point tracing the cycloid: the inner boundary of the generated shape provides the perimeter of a cycloidal gear (Figure 9). A different gear can be obtained by moving the tracing point inside the rolling circle: the obtained perimeter defines a contracted cycloidal gear, which presents a smoother boundary with respect to an ordinary cycloid (Figure 10). The coupling between the cycloidal disk and the fixed ring is achieved by substituting the ring with a number $N > n$ (where n is the number of lobes of the gear) of pins, placed equally spaced along the inner circumference of the ring (called roller Pitch Circle Diameter).

An important aspect is that the transmission ratio i of the adopted cycloidal disk depends only on the number of lobes n and on the number of pins N accordingly to the following definition:

$$i = \frac{n}{N - n} \quad (6)$$

The design of this kind of gear is due to O. Younis [12]: he provided the parametric equations used to shape

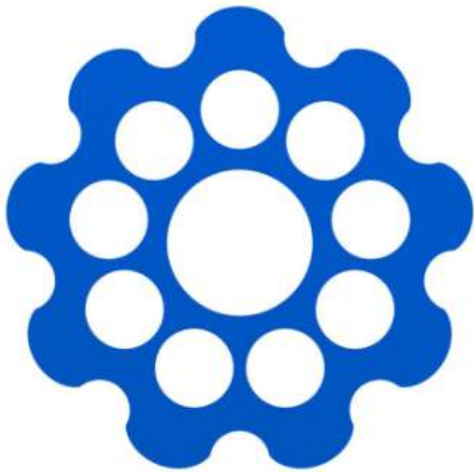


Figure 9: Ordinary cycloidal gear.

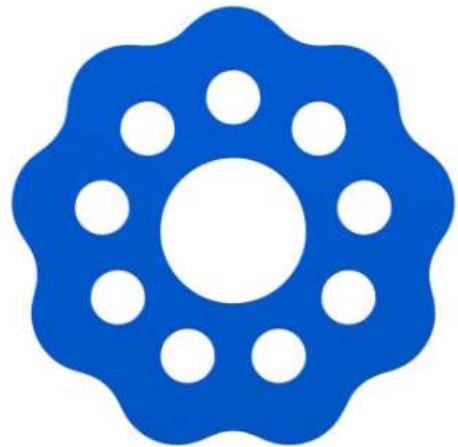


Figure 10: Contracted cycloidal gear.

a contracted cycloidal gear characterized by a number of lobes $n = N - 1$. Once that it has been defined the radius of the rollers as R_r , the radius of the rollers PCD as R and the eccentricity of the cycloidal gear axis as E , the profile of the gear is defined through the parameter t (going from 0 to 360) as:

$$x(t) = (R \cdot \cos(t)) - R_r \cdot \cos \left[t + \operatorname{atan} \frac{\sin((1-N) \cdot t)}{\frac{R}{E \cdot N} - \cos((1-N) \cdot t)} \right] - (E \cdot \cos(N \cdot t)) \quad (7)$$

$$y(t) = -(R \cdot \sin(t)) + R_r \cdot \sin \left[t + \operatorname{atan} \frac{\sin((1-N) \cdot t)}{\frac{R}{E \cdot N} - \cos((1-N) \cdot t)} \right] + (E \cdot \sin(N \cdot t)) \quad (8)$$

The final result is a cycloidal transmission composed of several elements (Figure 11):

1. The contracted cycloidal gear characterized by n lobes;
2. The input shaft, presenting an eccentricity E in correspondence of the gear;
3. N fixed pins placed along the PCD;
4. an arbitrary number of pins integral with an output plate.

This system still presents some issue. First of all, the presence of a single gear could introduce vibrations in the system. In order to solve this issue, two cycloidal gears with the same shape but aligned along the input shaft with a phase difference of 180 can be implemented in the model: in this way the unbalanced forces are naturally compensated and higher torques can be transmitted reducing at the same time mechanical issues due to unbalanced stresses (in particular, bending of the input axis and output pins). A second problem arises when mechanical resistance is considered: very high forces are exerted on the component of the transmission, in particular on the fixed pins and on the external case. However, being the reduction ratio only dependant by the number of fixed pins and lobes of the cycloidal gear, some flexibility on the sizing of the elements is available, providing the possibility to find the correct balance between encumbrance and mechanical resistance (Figure 12).

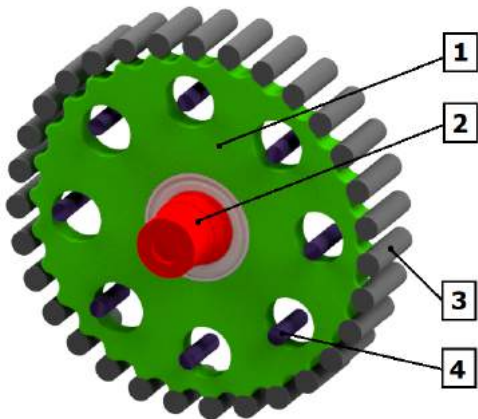


Figure 11: Section view of the assembled cycloidal transmission:

- 1) Cycloidal gear;
- 2) Input shaft with eccentricity;
- 3) Fixed pin;
- 4) Output pin.

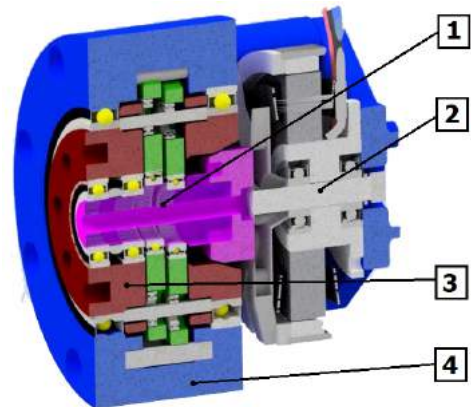


Figure 12: Section view of the assembled cycloidal transmission:

- 1) Cycloidal gear system;
- 2) Brushless motor;
- 3) Output plate;
- 4) External case.

2.2.4 Comparison and selection of the reduction

The actuator for our low-back exoskeletons needs to fulfill the following requirements:

- Backdrivability;
- Compact dimensions;
- Low cost;
- High efficiency;
- Long lasting.

Commercial solutions have already been discarded: even though the performances are remarkable, the cost of these devices would bring to an increase in manufacturing costs.

As for the custom solutions, the planetary gears presents some disadvantages. In the first place, the inability to realize a single-stage reduction will results in a critical drop in efficiency. In addition to this, the manufacturing of the gears is critical: the small dimension of the teeth prevents the manufacturing of the gears by means of filament 3D printer. It is also necessary to point out that these components should be characterized by extraordinary mechanical properties: in particular, since the motor torque flows towards the output carrier passing through the sun gear, the stresses generated on this component are rather high. A first esteem of the stresses exerted on the transmission can be performed through a Finite Element Analysis (see Section ?? for the detailed procedure): in Figure 13 it is possible to appreciate that, with an input torque of 1Nm, the sun gear has to withstand stresses higher than 50 MPa. For this reason, alternative manufacturing solutions should be considered, like the 3D-printing through laser sintering of polymers (e.g., Nylon P2200): laser printers like EOS Formiga 110 Velocis by SLS are capable of producing small components, guaranteeing both high mechanical properties and very high dimensional precision. On the other hand, this kind of printing technology is rather expensive, in particular, if compared with filament 3D printing.

On the other hand, cycloidal transmissions guarantee a longer operating life, low backlash, and higher torsional

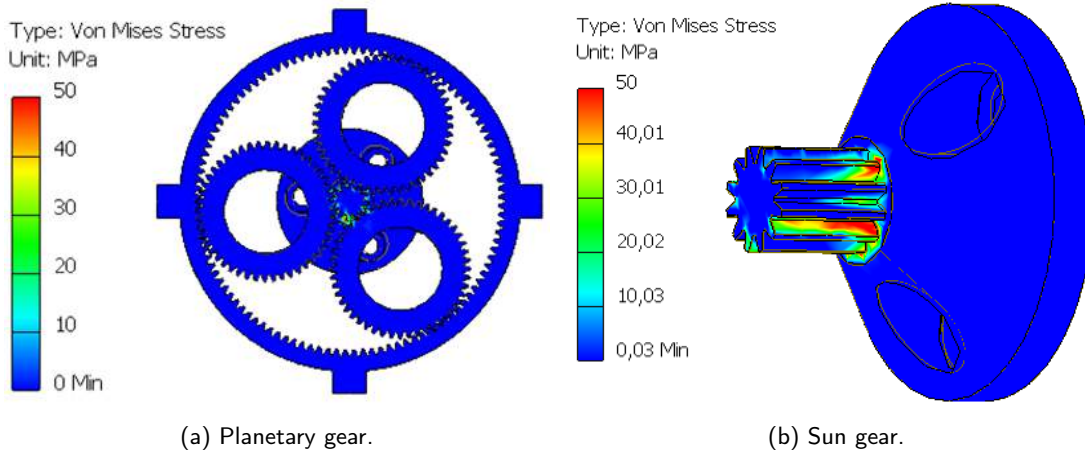


Figure 13: FEM analysis for planetary gear.

stiffness if compared with the previous custom reduction. Moreover, all the components can be printed through filament extrusion, drastically reducing manufacturing costs. Unfortunately, it is impossible to create a custom transmission as reliable as the commercial ones because of the material used, the technology adopted, and the design developed in years of expertise. However, it is possible to prototype a cycloidal transmission focusing on a design characterized by low maintenance costs (i.e., spare parts easy to get/realize and replace), reducing the impact of the reliability of the custom reduction.

3 MECHANICAL DESIGN

The low-back exoskeleton presents some base components which must be properly designed in order to guarantee the functioning of the device:

- 2 scissor hinges, already presented in Section 2;
- 2 actuating systems, one for each hinge;
- 1 hip support;
- 1 control board case;
- 1 battery;
- 2 user-exoskeleton interfaces, one at the low back, one at the upper-back.

3.1 General Constraints

During the prototyping phase of the exoskeleton it must be paid attention both to the constraints provided by the scissor hinge (the only element to be preserved from the initial design) and to the manufacturing method. The couple of scissor hinges must keep a distance of 115 mm from each other and be anchored to the hip support by means of two fixed pins (interaxle spacing of 45 mm).

As regards the custom elements, they are realized through filament extrusion 3D printing (Flashforge Creator 3 fed with Nylon PA12+CF15 by Fiberlogy [Table 1]), guaranteeing high flexibility while designing complex shapes. However some constraints are to be considered: first of all the volume of each piece must be reduced at the minimum value that allows the required mechanical properties while limiting the weight of the overall

Table 1: Mechanical Properties of Nylon PA12+CF15 filament [5].

bluePoli40	Test method	Unit	Typical Value
Tensile Strength @Yield	ISO 527	MPa	N/A
Tensile Strength @Break	ISO 527	MPa	120
Tensile Modulus	ISO 527	MPa	7300
Elongation @Yield	ISO 527	%	N/A
Elongation @Break	ISO 527	%	5
Flexural Strength	ISO 178	MPa	N/A
Flexural Modulus	ISO 178	MPa	7000
Izod Impact Strength (Notched) @23C	ISO 180	kJ/m ²	15

assembly, the printing time and its cost. Also the orientation of the printing layers has to be considered in the design, not only to reduce the support material to be created but also to maximize the mechanical properties (which are not isotropic) in the direction undergoing to higher stresses. In particular, the mechanical resistance represents a critical issue: besides the effect caused by the presence of the layers, even the mechanical properties of the material are different inside the same component due to manufacturing conditions that are impossible to be fully control (e.g. fluctuating temperature of the material when extruded, cooling rate, possible printing defects), forcing to shift towards a precautionary design aimed to avoid failures: increased width of stressed elements, higher radius fillets, removal of notches, . . .

Also, for the commercial components (e.g., fasteners, nuts, steel plates), the mechanical properties and their cost must be taken into consideration while choosing between different options. Moreover, the combination with the 3D printed elements has to be properly studied: not only it's necessary to define the coupling method but it is also important to guarantee a sufficient level of comfort during the assembly.

To achieve the best results, multiple FEM iterations of the prototyping were performed on all the components, in order to achieve a design capable to guarantee the functioning of the exoskeleton while preventing failures from occurring, reducing the weight and the encumbrance of the device, and guaranteeing a minimum level of comfort both during the assembly and the usage of the apparatus.

3.2 Cycloidal Drive Actuator

The actuating system has to be defined in order to proceed with the prototyping of the first prototype of the cycloidal gear providing a reduction 30:1 (Figure 14a). The first version, based on the reduction already presented in Section 2, is characterized by the following elements:

1. a brushless motor mj5208 by MJBots;
2. 2 cycloidal gears characterized by 30 lobes;
3. the input eccentric shaft, constrained to the motor;
4. 31 fixed pins;
5. an external case, divided in two parts design to constrain the fixed pins to their position, which can be used to fix the whole actuation system to the hip joint;
6. 2 rotating plates, axial to the shaft, integral with the pins pushed by the cycloidal gears;
7. a mounting for the motor, fixed to the external case in order to guarantee the necessary torque reaction;

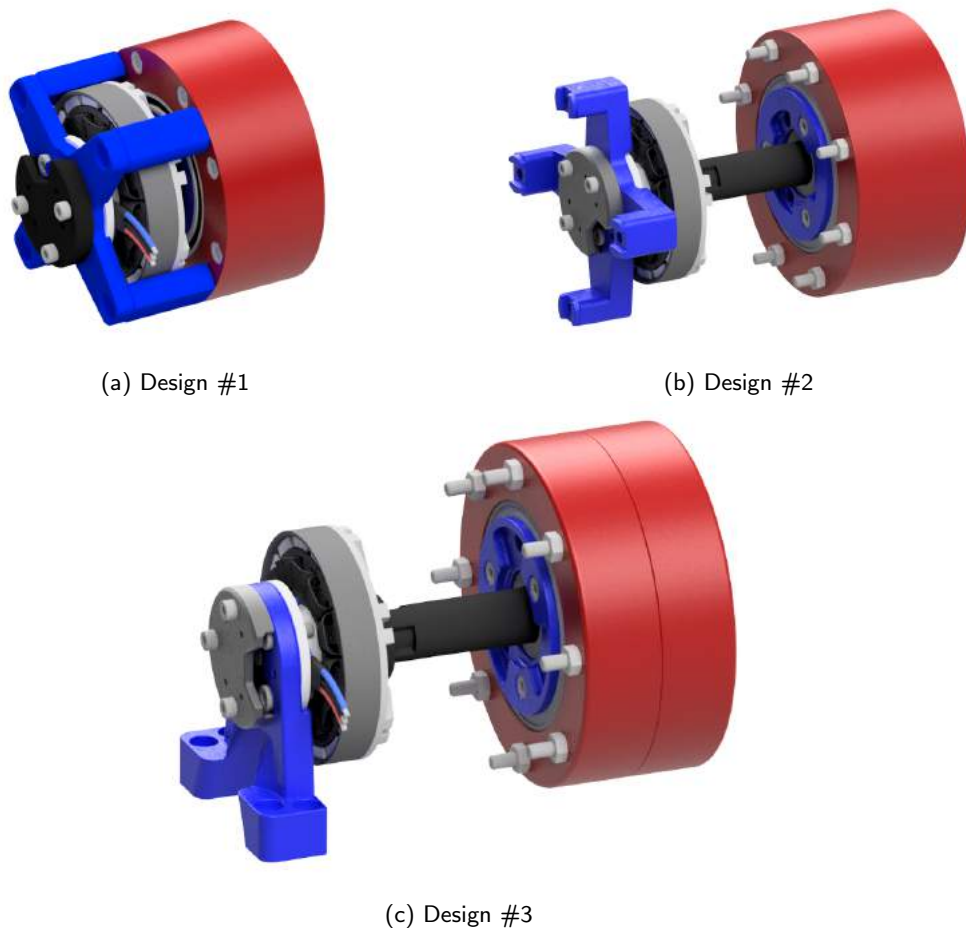


Figure 14: Design iterations for the actuation system.

8. an absolute magnetic encoder (AS5047P by AMS) and its case, both screwed to the motor mounting to be able to measure the motor axis position.
9. low-friction roller bearings to reduce internal losses and bolts and nuts to join firmly the assembly.

The current design has a total volume of $80 \times 80 \times 75 \text{ mm}^3$. Both the plates of point 6) could act as the output plates of the system; however, the one facing the motor is caged by the motor mounting, preventing it from being used as the output of the system. Using this design, being the actuation system directly connected to one of the fixed pins of a scissor hinge by means of the plate opposite to the motor, the actuation system could be mounted only externally with respect to the hinges: between the scissors, there is no sufficient space to mount two reduction system, since a space of 150 mm is required (vs the 115 mm available). This solution results in the device increasing its encumbrance to a maximum of 310 mm: even though the symmetry of this mounting does not cause the device to be too much uncomfortable, it could be interesting to re-design the actuation assembly in order to exploit the free space left between the scissor.

In order to achieve this result, the mounting of the motor can be detached from the reduction case and developed in order to be mounted directly on the hip joint. With this stratagem, the rotating plate facing

the motor can be freely connected to the first element of the scissor, allowing the actuation system to extend itself asymmetrically with respect to the scissor mechanism: the reduction is mounted on the external part (minimum total encumbrance reduced to 240 mm) while the motor, its mounting and the encoder (total length of about 30 mm) occupy the free space available on the inside (Figure 14b).

As for the anchoring of the motor mounting, the first solution consists in keeping the basic cross-shape of the first version, creating some spacers in the direction opposite to the motor: this spacer can be used to screw the mounting on a vertical panel integral with the hip joint. This solution presents the advantage of being rather solid and symmetric to the stresses. Nevertheless, two problems arise. The first one is represented by the fixing face, which requires more material to be realized (and more costs related to material and printing time), while the second one is related to the assembly of the system: the space available to screw firmly the two mounting to the central panel is very small, making the assembly pretty uncomfortable (in particular during the testing phase, when it is required to disassemble the motor to perform calibration and maintenance). In order to overcome these issues, a third prototype has been developed: a circular plate, required to fix the motor, is screwed to the hip joint by means of two supports. Even though the symmetry previously provided in transmitting the reaction force to the hip joint is lost, this support can be designed sufficiently thick to prevent bending in the direction tangential to the motor axis (Figure 14c). The bending in the axial direction instead represents a new issue, since it can cause vibrations of the motor, which could bring to a runout of the system or to a failure due to fatigue. This obstacle can be quickly overcome by adding a spacer between the motor mounting of the two actuating systems: since the bending of a motor mounting towards its reducer is constrained by the shaft (let's remember that the reducer will be constrained to the hip joint), the bending in the opposite direction is now constrained by the other actuation system, limiting the vibration of the system.

3.3 Hip Support

The hip support is a structural component and it is the "grounded" element of the device, the one which is integrally constrained to the low-back of the user and which provides anchor points for the other parts of the system.

The central piece acts as an anchoring base for the motor mounting and for the fans' detachable support, the design of which was also modified to reduce the encumbrance and to maximize the airflow to the motor coils (Figure 15). The junction of the three components has been achieved by means of several steel plates (AISI 304, thickness 2mm): on the bottom part, a large plate has been screwed into the elements at different points, guaranteeing their correct positioning. Similarly, on the top two narrow steel pieces were added to improve the mechanical resistance to bending. The removal of a large portion of the material to allow a comfortable mounting of the steel plates on the top part of the hip support causes the element to become too thin and excessively subjected to the high bending moments, which it must withdraw. Moreover, the new solution for the cooling system of the motors is still rather inefficient due to the small gap between the two fans (only 8 mm are available) which does not guarantee a sufficient flow of air to reach both fans; moreover, this simple anchoring constrains the fans only in the bottom part causing vibrations to happen and increasing the risk of contact between them and the actuation system.

In order to guarantee a proper coupling between the hip support and the actuation system the design of the motor mounting requires a further iteration. One of its support brackets, the one close to the low back of the user, is shortened in order to move its anchoring point on the top of the volume added on the hip support. As regards the cooling fans, a new solution has to be found. Since they do not introduce high stress on the exoskeleton, a support frame has been designed to be mounted on the rear, directing the airflow to the side of the motor: since no obstacles are placed beside the fans, the issue caused by the lack of air passing through the rotors is overcome. Even though this solution could be sub-optimal because of the cooling system not being directly aimed towards the coils of the motors, its effect could be enhanced by using at the same time two fans to cool down each motor: in fact the frame can be designed to follow the curvature of the motor,

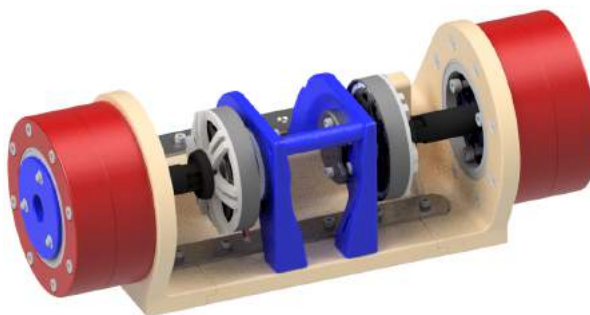


Figure 15: Mounting of the actuation system on the hip support.

so that the fans can be mounted stacked one above the other one while keeping their axes directed to the motors, doubling the cooling effect.

4 ASSEMBLY OF THE EXOSKELETON

The assembly of the exoskeleton and the final location on the user are shown in Figure 16.

The feasibility of the assembly has to be validated through a step-by-step simulation of the exoskeleton building to guarantee the coupling of all the elements.

The first step consists in assembling the three elements of the hip support by screwing the metal plate on the bottom part; then the connection with the low-back interface is achieved by exploiting the L-shaped metal components. Finally, the base structure is definitely reinforced by screwing the narrow steel plates on the upper part. The next step is the assembly of the two reductions, adding also the input shaft, which could be immediately mounted on the hip support by means of 8 screws, used to close the transmission case and to bind them to the base at the same time. The connection element between the reducer and the scissor is then mounted along the shaft and constrained to the output plate.

The BL motor and the encoder are then fixed to the motor mounting, but its connection to the hip support is not so trivial: there is no way to screw the input shaft to the motor because of the little space available in the assembly. For this reason, a small plate with a groove is screwed at the output of the motor: this groove perfectly meshes with the terminal shape of the input shaft, allowing the coupling by sliding the motor in the axial direction. Once in position, the motor mounting is screwed into the hip support and the spacer is added between the two mounts, locking the motor/shaft connection.

On the bottom part is now possible to screw the ODrive case into the hip support while installing the wiring to the motor, to the encoder, and towards the battery, mounted right behind the control board by means of high-strength Velcro.

The next step is the connection of the scissor hinges to the pins on the hip joint and to the actuated articulations connected to the reductions. On the terminal part of the hinges, the brackets of the upper-back user-exoskeleton interface are mounted. Finally, the harness can be constrained to the exoskeleton by means of the indented plates.

4.1 Kinematic Validation

Once the assembly of the exoskeleton has been verified as feasible, the correct working of the exoskeleton needs to be validated. This process is rather simple for our single DoF exoskeleton.

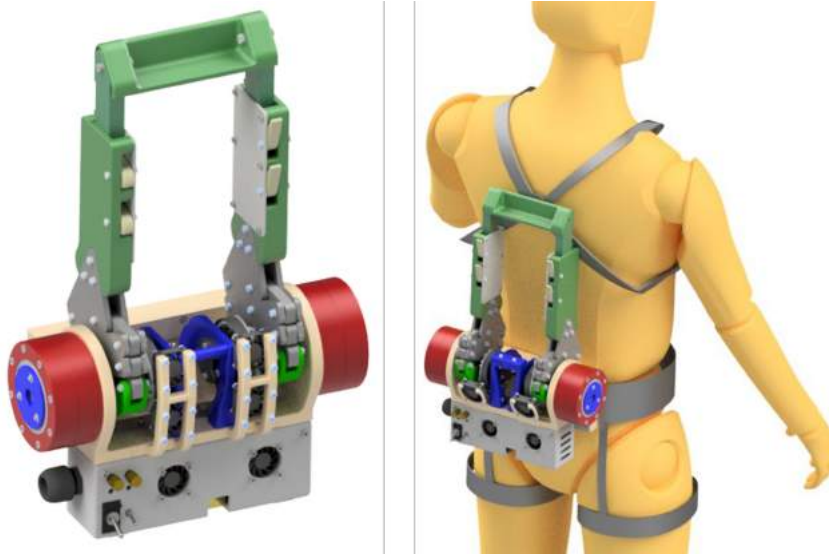


Figure 16: Exoskeleton assembled.

The kinematic validation is performed by simulating the actuation of the motor: an angular constraint is placed between the symmetry plane of the motor and the horizontal plane of the assembly. By increasing the value of the constraint by a fixed value, it is possible to analyze the behavior of the exoskeleton. For each increment, both a visual and a software analysis are performed. The preliminary visual analysis, already performed during the design process, is aimed at verifying the correct kinematic of the exoskeleton (in particular, the scissor hinges functioning) and identifying the presence of major unfeasibilities (i.e., permeation between the components). The software analysis consists of exploiting the command "Analyze interference" provided by Inventor: by selecting the whole assembly, the software is capable of quickly identifying the presence of hidden or very small interferences, not identifiable only with the visual inspection.

If an interference is identified, it must be promptly removed in order to guarantee the correct functioning of the device.

5 CONCLUSIONS

The proposed work presented the design methodology for a custom back-drivable cycloid transmission and its implementation on a new active back-support exoskeleton, based on backbone kinematics.

After a first overview of a passive low-back exoskeleton and its operative principle, it has been defined the main requirements for the definition of an actuator aimed to integrate an active control-compliant for the assistive device: back-drivability, high performance, and low cost. All the requirements were met with the design of a custom cycloidal reducer. The newly defined actuating system has been integrated into the low-back exoskeleton prototype by performing several design iterations of its components in order to achieve a compliant human-robot interaction. Finally a validation of the final model has been performed, both evaluating the kinematic of the device and simulating the mechanical response.

The result of this process is a new design for an active low-back exoskeleton whose main advantage is found in its scalability: by modifying the dimensional parameters of some elements (i.e. reduction, scissor hinge, and upper-back interface) it is possible to re-design a relatively short time an assistive device capable

to fully adapt to the anthropometry of the final user, enhancing the overall efficiency, before starting the manufacturing phase.

REFERENCES

- [1] A. Gupta, V.P.C.B., M.K. O'Malley: Design, control and performance of ricewrist: A force feedback wrist exoskeleton for rehabilitation and training. *The International Journal of Robotic Research*, 27, 2008. <http://doi.org/10.1177/0278364907084261>.
- [2] A. Zeiaee, R.L.R.T., R. Soltani-Zarrin: Design and kinematic analysis of a novel upper limb exoskeleton for rehabilitation of stroke patients. *International Conference on Rehabilitation Robotics*, 2017. <http://doi.org/10.1109/ICORR.2017.8009339>.
- [3] Bogue, R.: Exoskeletons and robotic prosthetics: a review of recent developments. *Industrial Robot*, 421–427, 2009. <http://doi.org/10.1108/01439910910980141>.
- [4] C.C. Gordon, C.C.B.B.J.M.I.T.R.W., T. Churchill: Anthropometric survey of us army personnel: Summary statistics, interim report for 1988. Tech. rep., Anthropology Re-search Project Inc., Yellow Springs OH, 1989.
- [5] Fiberlogy: Technical data sheet - nylon pa12+cf15, 2021. https://c-3d.niceshops.com/upload/file/FIBERLOGY_NYLON_PA12CF15_TDS.pdf.
- [6] L. Roveda, M.R.M.C.R.A.P.F.B.M.G., M. Pesenti: User-centered back-support exoskeleton: Design and prototyping. *Procedia CIRP*, 107, 522–527, 2022. <http://doi.org/10.1016/j.procir.2022.05.019>.
- [7] L. Roveda, S.A.T.D.G.L.L.M.T., L. Savani: Design methodology of an active back-support exoskeleton with adaptable backbone-based kinematics. *International Journal of Industrial Ergonomics*, 79, 2020. <http://doi.org/10.1016/j.ergon.2020.102991>.
- [8] R. Riener, I.M.G.C.V.D., L. Lnenburger: Locomotor training in subjects with sensori-motor deficits: An overview of the robotic gait orthosis lokomat. *Journal of Healthcare Engineering*, 5, 2010. <http://doi.org/10.5167/uzh-34694>.
- [9] Rubinshtein, M.: Cyberdyne bringing hal cyborg exoskeleton to us market, 2018. <https://www.knobbe.com/news/2018/06/cyberdyne-bringing-hal-cyborg-exoskeleton-us-market>.
- [10] Tec-science: Derivation of willis equation (fundamental equation of planetary gears), 2018. <https://www.tec-science.com/mechanical-power-transmission/planetary-gear/fundamental-equation-of-planetary-gears-willis-equation/>.
- [11] Y.M. Pirjade, N.P.D.L.T.S.S.O., A.U. Kotkar: Human assistive lower limb exoskeleton. *Asian Journal of Convergence in Technology*, 1, 2019. <http://doi.org/10.3390/electronics11030388>.
- [12] Younis, O.: Building a cycloidal drive with solidworks. Tech. rep. <https://blogs.solidworks.com/teacher/wp-content/uploads/sites/3/Building-a-Cycloidal-Drive-with-SOLIDWORKS.pdf>.